ELSEVIER

Journal of Nuclear Materials 278 (2000) 207–211

journal of nuclear materials

www.elsevier.nl/locate/jnucmat

Computer simulation of Pu^{3+} and Pu^{4+} substitutions in zircon

R.E. Williford [a,*], B.D. Begg [b], W.J. Weber [a], N.J. Hess [a]

[a] *Pacific Northwest National Laboratory, PO Box 999, Mail Stop K2-44, Richland, WA 99352, USA*
[b] *ANSTO, Materials Division, PMB 1, Menai, NSW 2234, Australia*

Received 1 June 1999; accepted 30 August 1999

Abstract

Energy minimization methods were used in atomistic computer simulations to determine the energetics of Pu^{3+} and Pu^{4+} substitutions and interstitials in zircon, including the effect of ion size. The lowest energy was found for Pu_{Zr}^{4+} substitutions. The lowest energy for Pu^{3+} substitutions was found for the defect cluster $2Pu_{Zr}^{3+'} + V_O^{\bullet\bullet}$. Mean field calculations of unit-cell volumes for 8% Pu substitutions were in agreement with X-ray diffraction (XRD) data.

PACS: 61.80.-X; 61.80.AZ; 61.82.MS

1. Introduction

Recent X-ray absorption spectroscopy (XAS) studies [1–3] on Pu-doped zircon ($ZrSiO_4$) have revealed that the Pu is in the 3+ state, which is a result of the original sample preparation under reducing conditions in an argon atmosphere. More recent work [4] has confirmed that the Pu^{3+} converts to Pu^{4+} upon annealing in air. Corresponding changes in unit-cell volumes have been detected by X-ray diffraction (XRD). The larger relative ionic radius of the Pu^{3+} state ($Pu^{3+}/Zr^{4+} > Pu^{4+}/Zr^{4+}$) is expected to change the preferred mechanism for incorporation of these ions into the zircon matrix. The purpose of this paper is to investigate how Pu^{3+} and Pu^{4+} are incorporated into the zircon lattice, and to provide the theoretical basis for more detailed experiments that are planned.

2. Computational methods and interatomic potentials

The general utility lattice program (GULP) [5,6] was used to simulate the energetics and structures of perfect and defective lattices. GULP uses an energy minimization method based on the Born model, and is unique in its use of crystal symmetry to speed up calculations. Isolated defects in extended solids were addressed with the Mott–Littleton approximation [7], with Region 1 sizes of 350–450 atom cores. Ionic polarization was treated using the Dick–Overhauser shell model [8], including the important repulsion–polarization coupling that prevents excessive polarization. Elemental defect energies were calculated by standard methods [9,10], and subsequently used to calculate the energetics of more complex defect configurations that included charge neutrality.

The interatomic potentials employed for Zr–O, Si–O, and O–O were previously developed for zircon [11], and have recently been used to determine vacancy migration energetics [12]. The eightfold coordination of the Zr–O potential [13] matches that of Zr in zircon. Two new potentials were developed for Pu^{3+}–O and Pu^{4+}–O by fitting to the structures and available properties of Pu_2O_3 and PuO_2 [14,15], which also have eightfold coordination for the Pu. Results are shown in Tables 1 and 2. All potentials were rigid ion models with formal charges, except oxygen which had a shell charge of −2.207 and a core-shell spring constant of 2727 eV/nm^2. The Buckingham form was used for all potentials

$$E = A\exp(-r/\rho) - C/r^6. \quad (1)$$

* Corresponding author. Tel.: +1-509 375 2956; fax: +1-509 375 2186.
E-mail address: re_williford@pnl.gov (R.E. Williford).

0022-3115/00/$ - see front matter
PII: S0022-3115(99)00244-5

Table 1
Parameters for potentials used in this work

Potential	A, eV	ρ, nm	C, 10^{-6} eV nm^6
Si–O	1283.9073	0.03205	10.6616
Zr–O	958.8690	0.03760	0.0
O–O	22764.0000	0.01490	27.89
Pu^{3+}–O	3144.8413	0.03148	0.0
Pu^{4+}–O	806.4236	0.04141	0.0

Table 2
Comparison between experimental and calculated data for $ZrSiO_4$, Pu_2O_3, and PuO_2

Material/parameter	Experiment	Calculation
$ZrSiO_4$		
a, b (nm)	0.6607	0.6306
c (nm)	0.5982	0.6442
c_{11} (GPa)	4.230	4.502
c_{12} (GPa)	0.703	0.628
c_{13} (GPa)	1.490	1.778
c_{33} (GPa)	4.900	5.094
c_{44} (GPa)	1.130	1.129
c_{66} (GPa)	0.485	0.107
ε_0	8.3–9.0	10.58
Pu_2O_3		
a, b (nm)	0.3838	0.3833
c (nm)	0.5918	0.5921
c_{11} (GPa)	–	3.243
c_{12} (GPa)	–	2.247
c_{44} (GPa)	–	1.068
ε_0	–	6.32
PuO_2		
a, b, c (nm)	0.5397	0.5459
c_{11} (GPa)	4.306[a]	4.635
c_{12} (GPa)	1.284[a]	0.785
c_{44} (GPa)	0.673[a]	0.523
ε_0	21.03[a]	20.11

[a] Data are calculated [15].

The ionic size effect is implicit in the fitted potentials, as shown in Fig. 1. The potentials are in the correct relative order for interatomic separations greater than about 0.085 nm, and are thus valid for the range of the cation–oxygen bond distances in zircon (0.20–0.25 nm). For comparative purposes (because an eightfold coordinated Pu^{3+} ionic radius was not available), the sixfold coordinated ionic radii of Pu^{3+}, Pu^{4+}, and Zr^{4+} are 0.100, 0.086, and 0.072 nm, respectively [16].

3. Defect formation energies

The formation energies of elemental defects were computed using standard methods [9,10], and the results

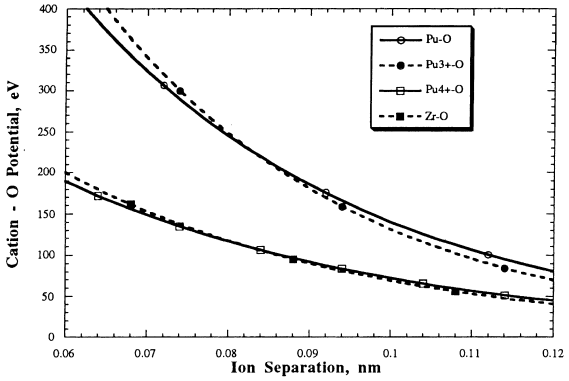

Fig. 1. Cation–Oxygen potentials. The curve Pu–O is from [11] for comparison.

are shown in Table 3 using Kroeger–Vink notation. The formation energies of the relevant lattices are also included in Table 3, and are denoted by the superscript L. The interstitial site with fractional coordinates (0.25, 0.0, 0.25) was used in this work because it had the lowest energy configuration, and is situated in the 'walls' of the channels when viewed along the [0 0 1] direction (e.g., Fig. 2 shows channels and walls).

Table 4 shows calculations for defect clusters ($2Pu_{Zr}^{3+\prime} + V_O^{\bullet\bullet}$ and $2Pu_{Zr}^{4+\prime}$) in several configurations, which are used in calculations in the next section. At minimum energy, the $2Pu_{Zr}^{3+\prime} + V_O^{\bullet\bullet}$ defect cluster forms the right-angle configuration shown by the black spheres in Fig. 2, with the oxygen vacancy near the center of the figure. This results in a polarized defect cluster with a slightly lower energy than the other two configurations considered, and significantly lower than the case for isolated point defects. The cluster $2Pu_{Zr}^{4+}$ has lowest energy when the two Pu substitutions reside on nearest neighbor Zr lattice sites. However, the right-angle configuration is only 0.02 eV/Pu higher, and could probably occur by thermal vibrations. Consequently, oxidation of the $2Pu_{Zr}^{3+\prime} + V_O^{\bullet\bullet}$ right-angle cluster could occur by filling

Table 3
Defect and lattice formation energies, eV

Defect or lattice	Energy
V_{Zr}''''	83.65
$V_O^{\bullet\bullet}$	21.05
O_i''	−14.43
$Pu_{Zr}^{3+\prime}$	37.75
Pu_{Zr}^{4+}	8.50
$Pu_i^{3+\bullet\bullet\bullet}$	−30.57
$Pu_i^{4+\bullet\bullet\bullet\bullet}$	−54.53
PuO_2^L	−101.45
$Pu_2O_3^L$	−131.82
ZrO_2^L	−109.69
$ZrSiO_4^L$	−475.66

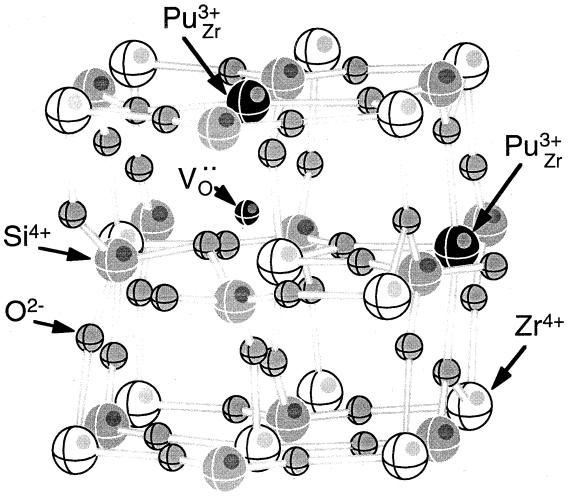

Fig. 2. The defect cluster $2Pu_{Zr}^{3+'} + V_O^{\bullet\bullet}$ in zircon, viewed along the [0 0 1] direction.

Table 4
Defect cluster formation energies, eV

Description	Energy
$2Pu_{Zr}^{3+'} + V_O^{\bullet\bullet}$ (rt. angle, 0.55 nm apart)	89.60
$2Pu_{Zr}^{3+'} + V_O^{\bullet\bullet}$ (near, 0.35 nm apart)	90.20
$2Pu_{Zr}^{3+'} + V_O^{\bullet\bullet}$ (linear, 0.63 nm apart)	90.76
$2Pu_{Zr}^{4+}$ (rt. angle, 0.55 nm apart)	17.14
$2Pu_{Zr}^{4+}$ (near, 0.35 nm apart)	17.10
$2Pu_{Zr}^{4+}$ (linear, 0.63 nm apart)	17.26

the oxygen vacancy to form the right-angle $2Pu_{Zr}^{4+}$ cluster, at an energy expense of only 0.07 eV/Pu higher than the single isolated Pu_{Zr}^{4+} defect.

4. Energies of Pu^{3+} and Pu^{4+} substitutions and interstitials with charge compensation

The most likely configuration of defects can be determined by writing the proper defect reaction equations and computing the resultant energies. Two approaches were taken for this, as follows. In the first approach, the perfect oxide lattices in Table 3 were taken as the reference states. This is a common approach for static energy minimization calculations, and often supplies a variety of possible defect reactions for consideration. In the second approach, the reference state was an 8 mol% Zr-deficient zircon lattice, into which 8 mol% Pu was substituted for Zr. This reference state reflects the stoichiometry of the experimental material. It should be noted that dilute Zr vacancies will not seriously affect the outcome of the defect reactions in the first approach.

4.1. Oxide lattice references

For the perfect oxide lattices as references, eight possible defect reactions are considered. The reactions and the corresponding defect energy equations are described below.

Reaction 1a. For isolated Pu^{3+} substitution on a Zr^{4+} site with charge compensation by an oxygen vacancy:

$$Pu_2O_3 + 2Zr_{Zr} + 4O_O \rightarrow 2ZrO_2 + 2Pu_{Zr}^{3+'} + V_O^{\bullet\bullet} + 4O_O, \tag{2}$$

$$E = 2ZrO_2^L + 2Pu_{Zr}^{3+'} + V_O^{\bullet\bullet} - Pu_2O_3^L = 8.99 \text{ eV } (4.50 \text{ eV/Pu}). \tag{3}$$

Reaction 1b. If neighboring defects are simulated as a cluster, and the defect formation energies from Table 4 are used for $2Pu_{Zr}^{3+'} + V_O^{\bullet\bullet}$, defect interactions significantly reduce the energy in Reaction 1a to 2.04, 2.64, and 3.20 eV (1.02, 1.32, and 1.60 eV/Pu) for the first three cases in Table 4, respectively. Thus, the incorporation of Pu^{3+} as a defect cluster on Zr sites as depicted in Fig. 2 represents the lowest energy configuration.

Reaction 2. For Pu^{3+} interstitials, with charge compensation by oxygen interstitials:

$$Pu_2O_3 \rightarrow 2Pu_i^{3+\bullet\bullet\bullet} + 3O_i'', \tag{4}$$

$$E = 2Pu_i^{3+\bullet\bullet\bullet} + 3O_i'' - Pu_2O_3^L = 27.39 \text{ eV} \quad (13.69 \text{ eV/Pu}). \tag{5}$$

Reaction 3. For Pu^{3+} interstitials, with charge compensation by Zr vacancies:

$$2Pu_2O_3 + 3Zr_{Zr} \rightarrow 3ZrO_2 + 4Pu_i^{3+\bullet\bullet\bullet} + 3V_{Zr}'''', \tag{6}$$

$$E = 1.5ZrO_2^L + 2Pu_i^{3+\bullet\bullet\bullet} + 1.5V_{Zr}'''' - Pu_2O_3^L = 31.62 \text{ eV} \quad (15.81 \text{ eV/Pu}). \tag{7}$$

Reaction 4. For mixed Pu^{3+} substitution on a Zr^{4+} site and Pu^{3+} interstitials, with charge compensation by zirconium vacancies:

$$2Pu_2O_3 + 3Zr_{Zr} + 3(4O_O) \rightarrow 3ZrO_2 + 2Pu_{Zr}^{3+'} + 2(4O_O) + 2Pu_i^{3+\bullet\bullet\bullet} + V_{Zr}'''' + 4O_O, \tag{8}$$

$$E = 1.5ZrO_2^L + Pu_{Zr}^{3+'} + Pu_i^{3+\bullet\bullet\bullet} + 0.5V_{Zr}'''' - Pu_2O_3^L = 16.29 \text{ eV} \quad (8.14 \text{ eV/Pu}). \tag{9}$$

Reaction 5a. For Pu^{4+} substitution on a Zr^{4+} site, no charge compensation is needed:

$$PuO_2 + Zr_{Zr} \rightarrow ZrO_2 + Pu_{Zr}^{4+}, \tag{10}$$

$$E = \mathrm{ZrO_2^L} + \mathrm{Pu_{Zr}^{4+}} - \mathrm{PuO_2^L} = 0.26\ \mathrm{eV} \quad (0.26\ \mathrm{eV/Pu}). \tag{11}$$

This is the lowest energy configuration for the incorporation of Pu^{4+}.

Reaction 5b. If two neighboring Pu_{Zr}^{4+} defects are simulated as a cluster, defect interactions produce energies of 17.14, 17.10, and 17.26 eV (0.33, 0.31, and 0.39 eV/Pu) for the last three cases in Table 4, respectively. These are only slightly higher than for isolated Pu^{4+} and are probably equally likely to occur.

Reaction 6. For Pu^{4+} interstitials with charge compensation by oxygen interstitials:

$$\mathrm{PuO_2} \rightarrow \mathrm{Pu_i^{4+\bullet\bullet\bullet\bullet}} + 2\mathrm{O_i''}, \tag{12}$$

$$E = \mathrm{Pu_i^{4+\bullet\bullet\bullet\bullet}} + 2\mathrm{O_i''} - \mathrm{PuO_2^L} = 18.06\ \mathrm{eV} \quad (18.06\ \mathrm{eV/Pu}). \tag{13}$$

Reaction 7. For Pu^{4+} interstitials, with charge compensation by zirconium vacancies (Frenkel-like):

$$\mathrm{PuO_2} + \mathrm{Zr_{Zr}} \rightarrow \mathrm{ZrO_2} + \mathrm{Pu_i^{4+\bullet\bullet\bullet\bullet}} + \mathrm{V_{Zr}''''}, \tag{14}$$

$$E = \mathrm{ZrO_2^L} + \mathrm{Pu_i^{4+\bullet\bullet\bullet\bullet}} + \mathrm{V_{Zr}''''} - \mathrm{PuO_2^L} = 20.88\ \mathrm{eV} \quad (20.88\ \mathrm{eV/Pu}). \tag{15}$$

Reaction 8. For mixed Pu^{4+} interstitials and substitutions on a Zr^{4+} site, with charge compensation by zirconium vacancies:

$$2\mathrm{PuO_2} + 2\mathrm{Zr_{Zr}} \rightarrow 2\mathrm{ZrO_2} + \mathrm{Pu_i^{4+\bullet\bullet\bullet\bullet}} + \mathrm{V_{Zr}''''} + \mathrm{Pu_{Zr}^{4+}}, \tag{16}$$

$$E = \mathrm{ZrO_2^L} + 0.5\mathrm{Pu_i^{4+\bullet\bullet\bullet\bullet}} + 0.5\mathrm{V_{Zr}''''} + 0.5\mathrm{Pu_{Zr}^{4+}} - \mathrm{PuO_2^L} = 10.57\ \mathrm{eV} \quad (5.29\ \mathrm{eV/Pu}). \tag{17}$$

Table 5 lists the energies of these defect reactions in order of decreasing preference, in terms of eV per Pu ion incorporated. As noted, Reaction 5a for Pu^{4+} incorporation and Reaction 1b for Pu^{3+} incorporation have the lowest energies, and should therefore be most likely to occur.

4.2. Zr-deficient zircon lattice reference

Using an 8 mol% Zr-deficient zircon lattice as the reference, there is only one valid defect reaction equation for each of the Pu^{4+} and Pu^{3+} substitution and interstitial scenarios. These four reactions are described below. Note that although Reaction 10 is different than Reaction 3 above, the conclusions are not changed.

Reaction 9a. For Pu^{3+} substitution on a Zr^{4+} site, with charge compensation by oxygen vacancies but not clustered:

$$\mathrm{ZrSiO_4} - 0.08\mathrm{ZrO_2} + 0.08\mathrm{PuO_{1.5}} \rightarrow \mathrm{Zr_{0.92}Pu_{0.08}^{3+}SiO_{3.96}}, \tag{18}$$

$$E = 0.08(\mathrm{Pu_{Zr}^{3+}} + 0.5\mathrm{V_O^{\bullet\bullet}} + \mathrm{ZrO_2} - \mathrm{PuO_{1.5}}) = 4.50\ \mathrm{eV/Pu} \quad (\text{same as Reaction 1a}). \tag{19}$$

Reaction 9b. If the defects in 9a are clustered, the result is

$E = 1.02$ eV/Pu

(same as Reaction 1b for the lowest energy configuration).

Reaction 10. For Pu^{3+} interstitials with charge compensation by zirconium and oxygen vacancies

$$\mathrm{ZrSiO_4} - 0.08\mathrm{ZrO_2} + 0.08\mathrm{PuO_{1.5}} \rightarrow \mathrm{(Zr_{0.92}\square_{0.08})Pu_{0.08i}^{3+}SiO_{3.96}}, \tag{20}$$

$$E = 0.08(\mathrm{V_{Zr}''''} + \mathrm{Pu_i^{3+\bullet\bullet\bullet}} + 0.5\mathrm{V_O^{\bullet\bullet}} + \mathrm{ZrO_2} - \mathrm{PuO_{1.5}}) = 19.83\ \mathrm{eV/Pu} \quad (\text{similar to Reaction 3}). \tag{21}$$

Reaction 11. For Pu^{4+} substitution on a Zr^{4+} site

$$\mathrm{ZrSiO_4} - 0.08\mathrm{ZrO_2} + 0.08\mathrm{PuO_2} \rightarrow \mathrm{Zr_{0.92}Pu_{0.08}^{4+}SiO_4}, \tag{22}$$

Table 5
Defect energies in terms of eV/Pu

Reaction	Description	eV/Pu
5a, 11	Pu_{Zr}^{4+} (isolated)	0.26
5b, 11	$2Pu_{Zr}^{4+}$ (cluster)	0.31, 0.33, 0.39
1b, 9b	$2Pu_{Zr}^{3+\prime} + V_O^{\bullet\bullet}$ (cluster)	1.02, 1.32, 1.60
1a, 9a	$2Pu_{Zr}^{3+\prime} + V_O^{\bullet\bullet}$ (isolated defects)	4.50
8	$0.5Pu_i^{4+\bullet\bullet\bullet\bullet} + 0.5V_{Zr}'''' + 0.5Pu_{Zr}^{4+}$	5.29
4	$Pu_{Zr}^{3+\prime} + Pu_i^{3+\bullet\bullet\bullet} + 0.5V_{Zr}''''$	8.14
2	$2Pu_i^{3+\bullet\bullet\bullet} + 3O_i''$	13.69
3, 10	$2Pu_i^{3+\bullet\bullet\bullet} + 1.5V_{Zr}''''$	15.81
6	$Pu_i^{4+\bullet\bullet\bullet\bullet} + 2O_i''$	18.06
7, 12	$Pu_i^{4+\bullet\bullet\bullet\bullet} + V_{Zr}''''$	20.88

$$E = 0.08(Pu_{Zr}^{4+} + ZrO_2 - PuO_2)$$
$$= 0.26 \text{ eV/Pu} \quad \text{(same as Reaction 5a)}. \tag{23}$$

Reaction 12. For Pu^{4+} interstitials with charge compensation by zirconium vacancies:

$$ZrSiO_4 - 0.08ZrO_2 + 0.08PuO_2$$
$$\rightarrow \quad (Zr_{0.92}\square_{0.08})Pu_{0.08i}^{4+}SiO_4, \tag{24}$$

$$E = 0.08(V_{Zr}^{''''} + Pu_i^{4+\bullet\bullet\bullet\bullet} + ZrO_2 - PuO_2)$$
$$= 20.88 \text{ eV/Pu} \quad \text{(same as Reaction 7)}. \tag{25}$$

5. Unit-cell volume changes

Several mean field calculations were performed (using partial occupancies of atomic sites in GULP) to check the volume changes associated with 8% Pu^{3+} or Pu^{4+} substitutions and associated oxygen vacancy compensation. The computed reference unit-cell volume for zircon was 0.25542 nm^3. For Pu^{3+} in Reaction 1a, the computed unit-cell volume was 0.26114 nm^3, which is in excellent agreement with the unit-cell volume (0.26224 nm^3) originally measured for this material [17]. For Pu^{4+} in Reaction 5a, the computed volume was 0.25858 nm^3. The relative values of these three computed volumes are also in excellent agreement with recent XRD data that will be reported elsewhere [4].

6. Conclusions

As expected, the lowest energy (0.26 eV/Pu in Reactions 5a and 11) was found for Pu_{Zr}^{4+} substitutions. This is consistent with the relative ease of synthesizing isostructural $PuSiO_4$. The lowest energy for Pu^{3+} reactions (1.02 eV/Pu in Reactions 1b and 9b) occurred for the defect cluster composed of two $Pu_{Zr}^{3+\prime}$ substitutions charge compensated by an oxygen vacancy. Mean field calculations of unit-cell volumes for 8% Pu substitutions agreed with XRD data.

Acknowledgements

This work was supported by the Environmental Management Science Program, Office of Environmental Management, US Department of Energy under Contract DE-AC06-76RLO 1830. The Pacific Northwest National Laboratory is operated by Battelle Memorial Institute for the US Department of Energy.

References

[1] N.J. Hess, W.J. Weber, S.D. Conradson, J. Nucl. Mater. 254 (1998) 175.
[2] N.J. Hess, W.J. Weber, S.D. Conradson, J. Alloys and Compounds 271–273 (1998) 240.
[3] N.J. Hess, W.J. Weber, S.D. Conradson, in: I.G. McKinley, C. McCombie (Eds.), Scientific Basis for Nuclear Waste Management XXI, Mater. Res. Soc. Symp. Proc., vol. 506, Materials Research Society, Warrendale PA, 1998, p. 169.
[4] B.D. Begg, N.J. Hess, W.J. Weber, S.D. Conradson, M.J. Schweiger, R.C. Ewing, this issue, p. 212.
[5] J.D. Gale, J. Chem. Soc., Faraday Trans. 93 (1997) 629.
[6] J.D. Gale, Philos. Mag. B 73 (1996) 3.
[7] N.F. Mott, M.J. Littleton, Trans. Faraday Soc. 34 (1938) 485.
[8] B.G. Dick, A.W. Overhauser, Phys. Rev. 112 (1958) 90.
[9] W. Hayes, A.M. Stoneham, Defects and Defect Processes in Nonmetallic Solids, Wiley, New York, 1985.
[10] R.E. Williford, R. Devanathan, W.J. Weber, J.D. Gale, J. Electroceramics, in print.
[11] Y. He, A.N. Cormack, J. Nucl. Mater., submitted.
[12] R.E. Williford, W.J. Weber, R. Devanathan, A.N. Cormack, J. Nucl. Mater. 273 (1999) 164.
[13] A. Dwivedi, A.N. Cormack, J. Solid State Chem. 79 (1989) 218.
[14] http//www.caos.kun.nl.
[15] C. Meis, J.D. Gale, Mater. Sci. Eng. B 57 (1998) 52.
[16] R.D. Shannon, Acta Crystallogr. A 32 (1976) 751.
[17] W.J. Weber, J. Mater. Res. 5 (1990) 2687.